# Hydrogenation Reactions of Ethylene on Neutral Vanadium Sulfide Clusters: Experimental and Theoretical Studies

Shi Yin, Yan Xie, and Elliot R. Bernstein*

Department of Chemistry, Colorado State University, Fort Collins, Colorado 80523-1872, United States

ABSTRACT: The reactions of C_2H_4 with H_2 on neutral vanadium sulfide clusters in a fast flow reactor are investigated by time-of-flight mass spectrometry employing 118 nm (10.5 eV) single photon ionization. The experimental products of these reactions are $V_mS_nC_2H_x$ ($m = 1$, $n = 1-3$; $m = 2$, $n = 1-5$, and $x = 4-6$). Observation of these products indicates that these V_mS_n clusters have high catalytic activity for hydrogenation reactions of C_2H_4. Density functional theory calculations at the BPW91/TZVP level are carried out to explore the geometric and electronic structures of the V_mS_n clusters and to determine

reaction intermediates and transition states, as well as reaction mechanisms. All reactions are estimated as overall barrierless or with only a small barrier (0.1 eV), and are thermodynamically favorable processes at room temperature. The ethylene molecule is predicted to connect with active V atoms through its π-orbital or form a σ-bond with active V atoms of catalytic V_mS_n clusters. The S atoms bonding with active V atoms play an important role in the dissociation of the H_2 molecule; H atoms transfer to the C_2H_4 (one after another) following breaking of the H—H bond. A catalytic cycle for C_2H_4 hydrogenation reactions on a vanadium sulfide catalyst surface is suggested based on our experimental and theoretical investigations.
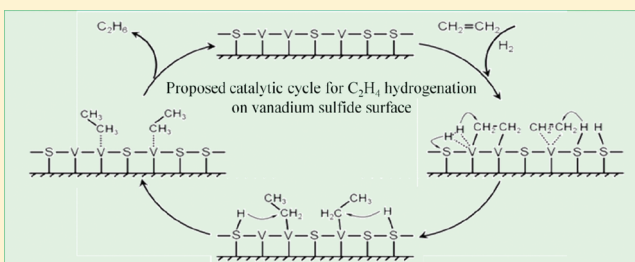
1. INTRODUCTION

Transition metal sulfides (TSMS) are of great significance in both industrial and biochemical catalysis.[1] The commercial use of TSMS catalysis is confined at present to heterogeneous systems, such as hydrogenation of unsaturated molecules, including aromatics, which is a mainstay of the petroleum and petrochemical industries.[2-5] The hydrogenation of ethylene by transition metal catalysts is one of the most widely studied reactions in heterogeneous catalysis[6-9] and numerous efforts have been devoted to these reactions for many years.[10-16] The ethylene reaction is a prototypical reaction for understanding the general mechanism of olefin and aromatic hydrogenation; it is particularly amenable to fundamental study.

Most studies of the mechanism of ethylene hydrogenation are focused on condensed phase systems[10-13] and transition metal surfaces.[17-26] The general mechanism for ethylene hydrogenation proposed by Horiuti and Polanyi in 1934 has been widely accepted.[27] According to their model, ethylene chemisorbs on the clean metal surface in either a di-σ or a π-bound configuration. Molecular hydrogen dissociatively coadsorbs over the metal to produce atomic hydrogen on the surface. Atomic hydrogen inserts into a metal—carbon bond to form an ethyl intermediate. The ethyl intermediate is hydrogenated by a second surface hydrogen atom to form ethane that subsequently desorbs into the gas phase. Many studies show that different surface species form and play different roles during the ethylene hydrogenation process on transition metal surfaces. For example, observation of ethylene hydrogenation on Pt(111),[13] monitored in situ using sum frequency generation indicates that π-bonded ethylene is

the primary intermediate in this system. Investigation of the reaction pathway for ethylene hydrogenation on Pd(111)[28] demonstrates that the addition of the first hydrogen atom to adsorbed ethylene to form an ethyl species is the rate-limiting step. Although a great deal is known about the basic elementary steps for ethylene hydrogenation from previous experimental and theoretical efforts, the mechanism of reaction on different catalysts at the molecular level still needs more investigation. Most assumed mechanisms focus on pure transition metal surfaces: no reaction mechanisms are proposed for hydrogenation of ethylene on transition metal sulfide surfaces or clusters, even though high catalytic reactivity is observed for many condensed phase TSMS catalyst.

Clusters in the gas phase can be good model systems for the simulation of real surface reactions and for the discovery of surface reaction mechanisms: clusters are readily accessible by theoretical techniques because they are isolated and their properties are localized. Gas phase studies of metal clusters and their reaction behavior can help to understand the mechanism of elementary reactions in catalytic processes under isolated, controlled, and reproducible conditions.[29-35] Vanadium group (5B) sulfides have been paid immense attention in the past few years. Condensed phase vanadium sulfides, particularly V_2S_3, are a good catalyst for hydrogenation reactions of various cyclic molecules.[36,37] Understanding metal sulfide catalytic chemistry at a molecular level starts with investigating the intrinsic properties of isolated metal sulfide clusters. Previous experimental work on gas phase

vanadium sulfide cation clusters (VS_n^+, $n = 1-10$) has employed various mass spectrometric methods and density functional theory (DFT) calculations.[38-42] The reactions of VS^+ with Xe, CO, COS, CO_2, and D_2 are studied using guided-ion beam mass spectrometry. Three product channels, formation of VS_2^+, V^+, and VO^+, were observed in the energy-dependent cross sections for the reaction of VS^+ with COS.[41] Cationic[43] and anionic[43,44] clusters with up to 14 vanadium atoms have been produced by laser ablation of vanadium/sulfur powder mixtures or V_2S_3 samples: $V_2S_2^+$, $V_3S_4^+$, and $V_4S_4^+$ are found to have relatively high stability. For neutral sulfide species, an earlier argon matrix study reacting transition metal atoms and OCS reported vibrations of VS and VS_2.[45] Spectroscopy of VS in the gas phase and VS_2 in an argon matrix can be found in refs 46 and 47, respectively.

In our previous work,[48] the distribution of neutral V_mS_n detected by single photon ionization (SPI) through 118 nm (10.5 eV) vacuum ultraviolet (VUV) laser radiation was reported. Vanadium sulfide clusters and hydrogen containing clusters ($V_mS_nH_x$, $x > 0$) are observed. With multiphoton ionization (MPI) through nanosecond UV (193 nm) radiation, V_mS_n clusters ($n > m + 1$) and hydrogen containing clusters cannot be observed, indicating severe fragmentation generated by MPI, and the importance of SPI in determining the neutral vanadium sulfide cluster distribution.

In the present work, hydrogenation reactions of ethylene on neutral vanadium sulfide clusters are studied by 118 nm SPI coupled with time-of-flight mass spectrometry (TOFMS). Detailed reaction mechanisms are suggested based on the experimental observations and DFT calculations. Based on the combined experimental and theoretical results, we present a proposed mechanism for ethylene hydrogenation facilitated by a vanadium sulfide catalyst surface.

2. METHODS

A. Experimental Procedures. The experimental setup for laser ablation coupled with a fast flow reactor employed in this work has been described previously in detail.[48-51] Only a brief outline of the apparatus is given below. V_mS_n clusters are generated by laser ablation of a mixed vanadium/sulfur target in the presence of a pure helium carrier gas (99.99%, General Air). The target is made by pressing a mixture of vanadium (99.5%, Sigma Aldrich) and sulfur (99.98%, Sigma Aldrich) powders. A 10 Hz, focused, 532 nm Nd^{3+}:YAG laser (Nd^{3+}: yttrium aluminum garnet) with 6 mJ/pulse energy is used for the laser ablation. The expansion gas is pulsed into the vacuum by a supersonic nozzle (R. M. Jordan, Co.) with a backing pressure of typically 75 psi. Generated vanadium sulfide clusters react with reactants in a fast flow reactor (i.d. 6.3 × 76 mm), which is directly coupled to the cluster generation channel (i.d. 1.8 × 19 mm). The reactant gases, ethylene (99.5% Sigma Aldrich) seeded in a pure helium or hydrogen gas, with a 20 psi backing pressure, are injected into the reactor by a pulsed General Valve (Parker, Serial 9). Timing between the Jordan valve and the General Valve opening is optimized for the best product yields. The pressure in the fast flow reactor can be estimated as 14 Torr for the reaction, and the collision rate between vanadium sulfide clusters and helium is estimated at about 10^8 s^{-1}.[50] Reactants and products are thermalized to 300-400 K by collision after the reaction.[52] An electric field is placed downstream of the reactor in order to remove any residual ions from the molecular beam. The beam of

neutral reactants and products is skimmed into a differentially pumped chamber and ionized by a separated VUV laser beam (118 nm, 10.5 eV/photon). The 118 nm laser light is generated by focusing the third harmonic (355 nm, ~30 mJ) of a Nd^{3+}: YAG laser in a tripling cell that contains about a 250 Torr argon/xenon (10/1) gas mixture. An MgF_2 prism (Crystaltechno LTD, Russia, 6° apex angle) is placed into the laser beam to enhance separation of the generated 118 nm laser beam from the 355 nm input laser beam. After the near threshold ionization, photoions are detected by a TOFMS.

B. Calculational Procedures. Calculations of the structural parameters for neutral V_mS_n clusters and the hydrogenation reactions of ethylene on these clusters are performed employing density functional theory (DFT). All the calculations are carried out with Becke's exchange[53] and Perdew—Wang's[54] correlation (BPW91) functional coupled with a triple-ζ valence plus polarization (TZVP) basis set within the Gaussian 09 program.[55] The BPW91/TZVP method is capable of calculating a reasonably good structure for V_mS_n ($m \neq 0$), as we discussed before.[48] The enthalpies of formation for ethylene are also very well calculated at this level of theory. Binding energies between neutral V_mS_n and C_2H_4 are calculated at different typical association geometries to obtain the lowest energy structures of the $V_mS_nC_2H_4$ clusters. The calculations for the potential energy surfaces (PESs) of the hydrogenation reactions of ethylene on V_mS_n involve geometry optimizations of the reactants, intermediates, transition states, and products. Vibrational frequency calculations are further performed to confirm the global minima ground states and transition states, which have zero and one imaginary frequency, respectively. Additionally, intrinsic reaction coordinate (IRC) calculations are carried out to determine that an estimated transition state connects two appropriate local minima along the reaction pathway. Binding energies are calculated for a few species employing the Basic Set Superposition Error (BSSE) correction:[56,57] these corrections are found to be insignificant at the present level of theory.

3. RESULTS

A. Experimental Results. Figure 1 presents a typical TOF mass spectrum of neutral vanadium sulfide V_mS_n ($m = 1-7$, $n = 1-11$) clusters generated by laser ablation of a pressed vanadium/sulfur (mole ratio V/S = 4) powder target into a pure He carrier gas, and ionized by 118 nm laser radiation. This method is different from that used in our previous investigation,[48] in which V_mS_n clusters are generated by laser ablation of a vanadium metal foil in the presence of a helium carrier gas seeded with various concentrations of H_2S or CS_2. In that work, hydrogen and carbon containing clusters are also generated: H and C containing clusters are not present in the current TOFMS data for V/S pressed ablation targets and pure He expansion gas. In Figure 1, the most intense mass peaks for each vanadium sulfide series are VS, V_2S_2, V_3S_4, V_4S_4, V_5S_6, and V_6S_6. The relatively high V_mS_n signal intensities are at $n = m$ for $m = 1, 2, 4, 6$ and $n = m + 1$ for $m = 3, 5$. Under the presented conditions, both sulfur poor ($n \leq 2m + 1$) and rich ($n > 2m + 1$) clusters can be observed. Some pure sulfur clusters S_m and oxygen containing clusters $V_mS_nO_x$ are also observed, because sulfur powder is used as the sulfur source and a trace amount of oxygen impurity may be contained in the pressed powder target and carrier gas. Various other V/S ratio targets were also prepared and used in the experiment. The spectra are similar to the one shown in Figure 1 for V/S mole
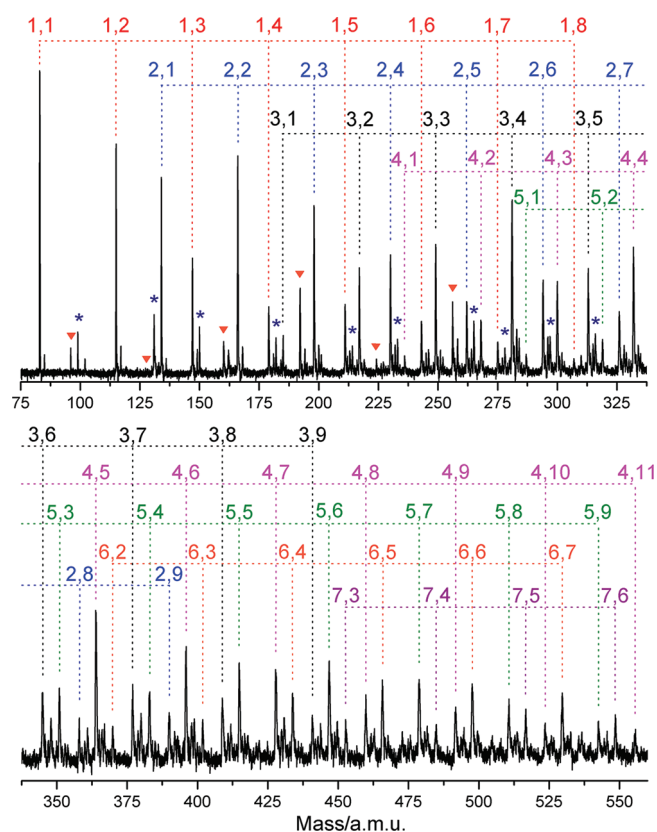
Figure 1. Neutral vanadium sulfide cluster V_mS_n ($m = 1-7$, $n = 1-11$) distribution detected by 118 nm single photon ionization and time-of-flight mass spectrometry. The series of pure sulfur clusters S_m ($m = 3-8$) are marked by a down triangle symbol, and the peaks marked with a star symbol are due to oxygen impurities. See text for details.
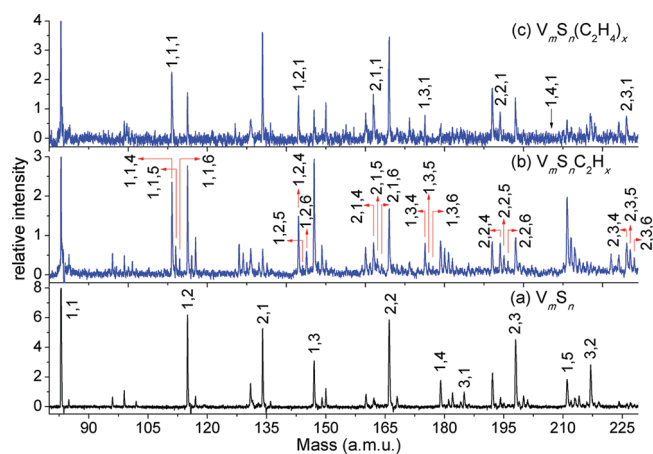

Figure 2. Neutral vanadium sulfide cluster V_mS_n ($m = 1, 2$; $n = 1-5$) distributions after reaction and collision with (a) pure helium; (b) 5% C_2H_4/H_2; (c) 5% C_2H_4/He in a fast flow reactor.

ratios in the range of 2–6. At low V/S ratios (V/S = 1), sulfur rich clusters and pure sulfur clusters S_m become a relatively more intense presence in the mass spectra. At high V/S ratios (V/S = 8), sulfur poor clusters become relatively intense and pure vanadium clusters, such as V_2, are observed.

Mass spectra generated from the reaction of neutral vanadium sulfide clusters with 5% C_2H_4 seeded in hydrogen gas in a fast

Table 1. Qualitative Comparison of Neutral Vanadium Sulfide Cluster Distributions V_mS_n ($m = 1, 2$) and Observed Products Following Reaction with Pure He, 5% C_2H_4/He and 5% C_2H_4/ H_2 in the Reaction Cell

	Products with different reaction gas	
Pure He	5% C_2H_4/He	5% C_2H_4/H_2
VS	VS	VS
	VSC_2H_4	VSC_2H_4
		VSC_2H_5
		VSC_2H_6
VS_2	VS_2	VS_2
		VS_2H
		VS_2H_2
	$VS_2C_2H_4$	$VS_2C_2H_4$
		$VS_2C_2H_5$ $(w)^a$
		$VS_2C_2H_6$
	$VS_2(C_2H_4)_2$	$VS_2(C_2H_4)_2$
VS_3	VS_3	VS_3
	$VS_3C_2H_4$	$VS_3C_2H_4$
		$VS_3C_2H_5$
		$VS_3C_2H_6$
VS_4	VS_4	VS_4
		VS_4H
		VS_4H_2
VS_5	VS_5	VS_5
		VS_5H
		VS_5H_2
VS_6	VS_6	VS_6
		VS_6H
VS_7	VS_7	VS_7
V_2S	V_2S	V_2S
		V_2SH
		V_2SH_2 $(w)^a$
	$V_2SC_2H_4$	$V_2SC_2H_4$
		$V_2SC_2H_5$
		$V_2SC_2H_6$
	$V_2S(C_2H_4)_2$	$V_2S(C_2H_4)_2$
V_2S_2	V_2S_2	V_2S_2
	$V_2S_2C_2H_4$	$V_2S_2C_2H_4$
		$V_2S_2C_2H_5$
		$V_2S_2C_2H_6$
V_2S_3	V_2S_3	V_2S_3
		V_2S_3H
	$V_2S_3C_2H_4$	$V_2S_3C_2H_4$
		$V_2S_3C_2H_5$
		$V_2S_3C_2H_6$
V_2S_4	V_2S_4	V_2S_4
		V_2S_4H
	$V_2S_4C_2H_4$	$V_2S_4C_2H_4^b$
		$V_2S_4C_2H_5$
		$V_2S_4C_2H_6$
V_2S_5	V_2S_5	V_2S_5
		V_2S_5H
	$V_2S_5C_2H_4$	$V_2S_5C_2H_4$
		$V_2S_5C_2H_5$

Table 1. Continued

| Pure He | Products with different reaction gas | |
	5% C_2H_4/He	5% C_2H_4/H_2
		$V_2S_5C_2H_6$
V_2S_6	V_2S_6	V_2S_6
		V_2S_6H

^{a} w in parentheses denotes the signal of intensity is weak. ^{b} Overlapped with $^{34}S_8$ in mass number.

flow reactor are presented in Figure 2b. By way of comparison, Figure 2a shows the TOFMS for V_mS_n clusters reacting with only He in the reaction cell, and Figure 2c shows TOFMS for V_mS_n clusters reacting with 5% C_2H_4/He in the reaction cell. The products for reactions of V_mS_n with C_2H_4 seeded in hydrogen and in helium gas are also compared qualitatively, as listed in Table 1. If pure He gas is added to the reactor cell, all cluster signals decrease in roughly the same proportion due to scattering by the inert gas in the reactor (Figure 2a). Figure 2c displays the mass spectrum of reactants and products for the reaction of V_mS_n clusters with C_2H_4. Many association products are observed when 5% C_2H_4/He is added to the fast flow reactor. Products $VS_{1-3}C_2H_4$ and $V_2S_{1-5}C_2H_4$ are readily detected; they are generated from the association reactions,

$$V_mS_n + C_2H_4 \rightarrow V_mS_nC_2H_4 \qquad (1)$$

and are stabilized (cooled) by third body (usually He) collisions (Table 1).

The reactions of V_mS_n clusters with C_2H_4 and H_2 generate two new cluster series: the adduct of both C_2H_4 and H_x to form the products $VS_{1-3}C_2H_x$, $V_2S_{1-5}C_2H_x$ (x = 5, 6); and the adduct of only H_x to form the products $VS_2H_{1,2}$, $VS_{4,5}H_{1,2}$, $V_2SH_{1,2}$, and so on (Figure 2 and Table 1). The general reactions are

$$V_mS_n + C_2H_4 + H_2 \rightarrow V_mS_nC_2H_6 \qquad (2)$$

$$V_mS_n + H_2 \rightarrow V_mS_nH_2 \qquad (3a)$$

$$2V_mS_n + H_2 \rightarrow 2V_mS_nH \qquad (3b)$$

Based on this behavior, these experimental results suggest that certain V_mS_n clusters are active with the C_2H_4/H_2 gas mixture and could be a catalyst for the ethylene hydrogenation reaction. For the products $V_mS_nC_2H_5$ and V_mS_nH, the additional hydrogen atoms to generate the ethyl radical might come from the dissociation of H_2 molecules in multiple cluster molecule collision reactions. To explore and elucidate this interpretation, the reaction energies, mechanisms, and potential energy surfaces for the $V_mS_n + C_2H_4 + H_2$ reaction system are calculated. Theoretical results can supply more information, as discussed in the next section.

B. Theoretical Results. To study the mechanism of ethylene hydrogenation with V_mS_n cluster species theoretically, DFT calculations are performed for the reactions $C_2H_4 + H_2 \rightarrow C_2H_6$ on VS_{1-3} and V_2S_2 clusters. Experimentally, the more product intensity for reactions $V_mS_n + C_2H_4$ compared to reactions $V_mS_n + H_2$ (Figure 2b) suggests that the interaction of V_mS_n with ethylene is much stronger than the interaction of V_mS_n with H_2. Pure H_2 gas in the fast flow reactor is also investigated as reference: hydrogen association products are not intense and not as stable as ethylene association products, as shown in

Figure 2c. This experimental result also suggests that V_mS_n clusters are more active with C_2H_4 than with H_2. DFT calculations yield that the association energy for C_2H_4 and V_mS_n is much larger than the association energy for H_2 and V_mS_n. For example, the association binding energies are 1.09 and 0.30 eV for C_2H_4 and H_2 with V_2S_2, respectively. Therefore, in a competitive environment, C_2H_4 will be preferentially adsorbed on vanadium sulfide clusters as the first step, rather than H_2, in the hydrogenation process.

The PESs and the optimized geometries of reaction intermediates and transition states calculated by DFT for the reactions $VS_{1-3} + C_2H_4 + H_2 \rightarrow VS_{1-3} + C_2H_6$ and $V_2S_2 + C_2H_4 + H_2 \rightarrow V_2S_2 + C_2H_6$ are presented in Figures 3−5 as typical examples. The quartet ground state for VS and the doublet ground state for VS_2 have the lowest energy, and the most stable adsorption structures are for both C_2H_4 and H_2 bonded to the vanadium atom in VS and VS_2 clusters. The hydrogen bond of the adsorbed hydrogen molecule can be broken on the V atom: one hydrogen atom remains bonded to the vanadium atom, while the other hydrogen atom transfers to the sulfur atom forming an -SH group (through **TS1** and **TS5** in Figure 3, respectively). Then hydrogen transfer reactions occur from the −VH group and the −SH group one by one for the overall hydrogenation reaction of ethylene. The mechanism is barrierless, as presented in Figure 3.

Figure 4 presents the reaction pathway for ethylene hydrogenation on a VS_3 cluster. C_2H_4 bonds to the V atom of VS_3 to form intermediate **I12**, and then the hydrogen molecule attacks the middle position of the two adjacent sulfur atoms to form intermediate **I13** via transition state **TS8**. Through transition states **TS9** and **TS10**, hydrogen atoms of the −SH groups transfer to ethylene and yield intermediate **I15**, for which one of the C atoms of ethane bonds to the V atom of VS_3. For the reaction mechanism study of ethylene hydrogenation on catalytically active V_2S_m series of vanadium sulfide clusters, DFT calculations are performed for the reaction on the V_2S_2 cluster, as shown in Figure 5. The lowest energy adsorption structure is found as intermediate **I17**. The C_2H_4 and H_2 molecules bond to the V atoms. Through transition state **TS11**, the H−H bond ruptures and yields intermediate **I18**, which contains −VH and −SH groups. The H atom of −VH group transfers to C_2H_4 and forms ethyl bonded to the other V atom. Then the H atom of −SH group transfers to the ethyl through transition states **TS13** and **TS14**: intermediate **I19** transforms to intermediate **I21**, in which ethane is attached to V_2S_2 by an association energy of ∼0.3 eV.

4. DISCUSSION

A. Association Reactions of V_mS_n with C_2H_4. According to surface science investigations[13,58−60] of ethylene hydrogenation, the association of ethylene to a catalytic metal surface is an important step. The metal surface generates several distinct surface species that can be monitored with a variety of techniques: one species is a π-bonded ethylene, in which ethylene associates with a metal site through its π-orbitals; another species is a di-σ-bonded ethylene, in which ethylene breaks the π bond and forms two σ bonds to the surface metal atoms; and a third species is ethylidyne (M≡CCH₃), in which ethylene dehydrogenates by transferring one hydrogen atom from one carbon to the other and losing one hydrogen. In our work, association reactions are found to be the main reaction for vanadium sulfide clusters with ethylene. As shown in Figure 2 and Table 1, $VS_{1-3}C_2H_4$ and
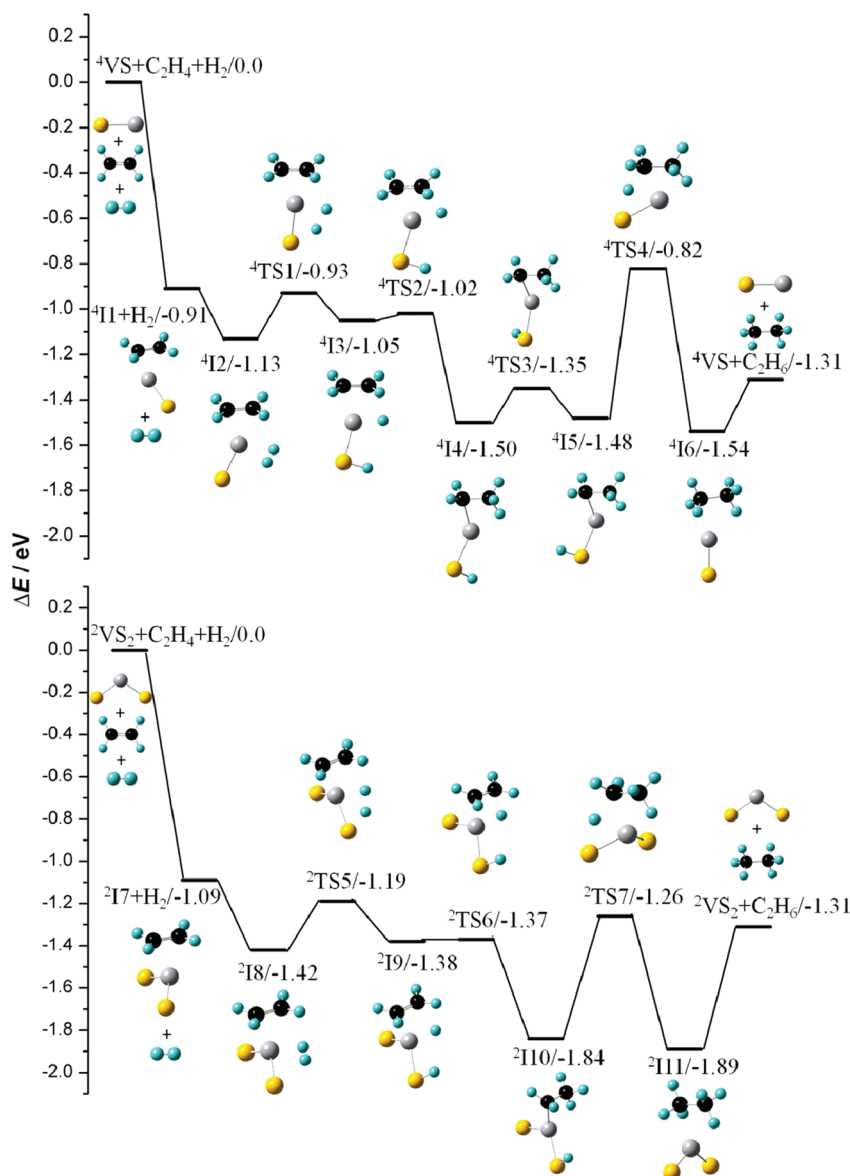
10269

dx.doi.org/10.1021/jp2056267 |J. Phys. Chem. A 2011, 115, 10266−10275

Figure 3. Reaction pathways for $^4VS + C_2H_4 + H_2 \rightarrow {}^4VS + C_2H_6$ and $^2VS_2 + C_2H_4 + H_2 \rightarrow {}^2VS_2 + C_2H_6$, calculated at the BPW91/TZVP level. The reaction intermediates and transition states are denoted as ^MIn and ^MTSn, respectively, in which the superscript M indicates the spin multiplicity. Energies, including ZPE corrections, are given in eV and are relative to the initial energy of the $^4VS + C_2H_4 + H_2$ and $^2VS_2 + C_2H_4 + H_2$ reactants, respectively. V atoms are gray, S atoms are yellow, C atoms are black, and H atoms are cyan.

$V_2S_{1-5}C_2H_4$ are the only products identified for reactions of V_mS_n with C_2H_4 seeded in helium gas (Figure 2c) and are the main products for C_2H_4 seeded in hydrogen gas (Figure 2b).

To understand the bond types for association of ethylene to V_mS_n clusters, the lowest energy structures of association products $V_{1,2}S_{1-3}C_2H_4$ are determined by DFT calculations and presented in Figure 6. Two types (π and σ) of typical configurations are found. In the π type configuration, two carbon atoms of C_2H_4 connect with one V atom through π-orbitals of ethylene. The C—C bond lengths in the π configuration (1.361–1.383 Å) are close to that of the double bond of the ethylene molecule (1.333 Å, calculated at the same level of theory): this structure also indicates that the π bond of ethylene is not broken. In the σ configuration, the π bond of ethylene ruptures as the C—C bond length increases to 1.463–1.483 Å (close to the single bond length of ethane 1.531 Å). One carbon atom of C_2H_4 bonds to

one V atom, and the other carbon atom connects with two V atoms of $V_2S_{1,2}$ clusters (see Figure 6). In the calculations, binding energies listed below each geometry are defined as $E(V_{1,2}S_{1-3}) + E(C_2H_4) - E(V_{1,2}S_{1-3}C_2H_4)$. As shown in Figure 6, the binding energy of ethylene with V_mS_n clusters of type σ (1.37–1.76 eV) is larger than that of type π (0.67–1.09 eV); but the difference of binding energy between π and σ types does not generate an important effect on the continuing hydrogenation reaction of ethylene, based on the PES calculational results presented in Figures 3–5. The ethylene in both π and σ configurations can be hydrogenated in a stepwise fashion through an ethyl intermediate to ethane following the reaction surface. These results suggest that π and σ type bound species are both available for ethylene to associate with catalytic V_mS_n clusters and that the ethylene of both binding types can be hydrogenated barrierlessly. These conclusions are in agreement with present observations, and
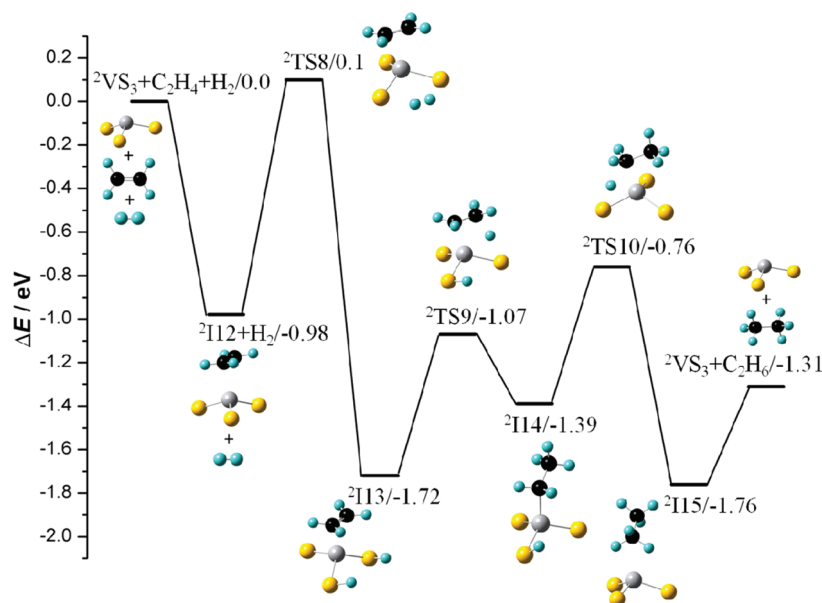
Figure 4. Reaction pathway for $^2VS_3 + C_2H_4 + H_2 \rightarrow {}^2VS_3 + C_2H_6$ calculated at the BPW91/TZVP level. Energies, including ZPE corrections, are given in eV and are relative to the initial energy of the $^2VS_3 + C_2H_4 + H_2$ reactants. See caption to Figure 3 for more explanation.

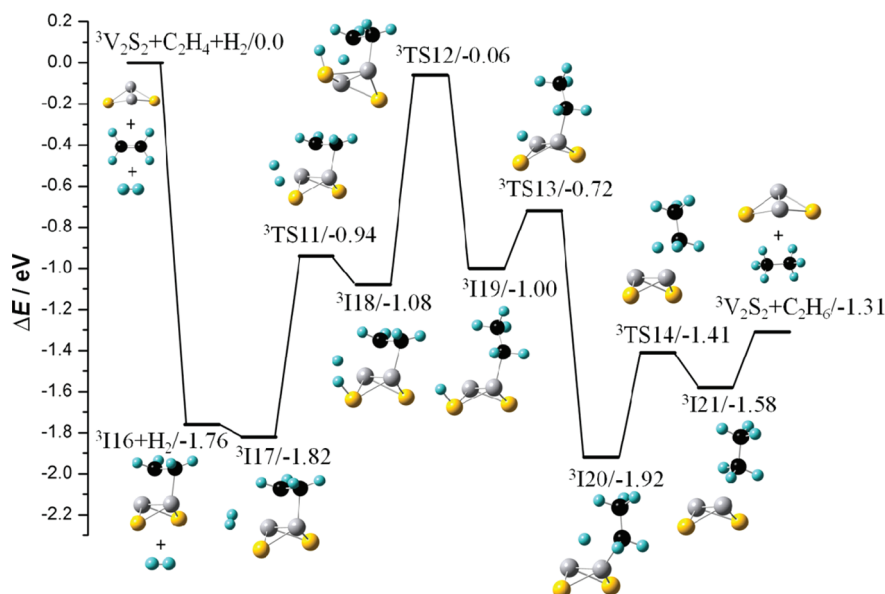**Figure 5.** Reaction pathway for $^3V_2S_2 + C_2H_4 + H_2 \rightarrow {}^3V_2S_2 + C_2H_6$ calculated at the BPW91/TZVP level. Energies, including ZPE corrections, are given in eV and are relative to the initial energy of the $^3V_2S_2 + C_2H_4 + H_2$ reactants. See caption to Figure 3 for more explanation.

the results of studies of ethylene hydrogenation on a Pt/Al$_2$O$_3$ catalyst surface.[61]

B. Hydrogenation Mechanism for $V_mS_n + C_2H_4 + H_2$ Reactions. In addition to C_2H_4 association products observed for the reaction of $V_mS_n + C_2H_4 + H_2$, new products, $V_mS_nC_2H_5$, $V_mS_nC_2H_6$ ($m = 1, n = 1-3; m = 2, n = 1-5$), and $V_mS_nH_x$ ($m = 1$, $n = 2, 4-6; m = 2, n = 1, 3-6; x = 1, 2$) can be observed in Figure 2b and Table 1. Although the position of mass peaks of $V_mS_nC_2H_6$ are overlapped with those of $V_m{}^{34}SS_{n-1}C_2H_4$, products $V_mS_nC_2H_6$ are clearly identified by comparison with mass spectra shown in Figure 2c, which only contain isotopic mass peaks $V_m{}^{34}SS_{n-1}C_2H_4$. For example, the intensity ratio of mass

peak 145 amu (corresponding to $V^{34}SSC_2H_4$ or $VS_2C_2H_6$) to 143 amu (corresponding to $VS_2C_2H_4$) is about 8%, as measured in Figure 2c, but in Figure 2b, that ratio increases to 40%: the increase of 32% for this ratio indicates that the association product $VS_2C_2H_6$ is generated. Molecular adsorption of C_2H_4 and H_2 on the V_mS_n cluster allows C_2H_6 to be formed from hydrogenation reactions that are thermodynamically and dynamically favorable at room temperature (see Figures 3-5 as examples). The observed products, $V_mS_nC_2H_6$ ($m = 1, n = 1-3; m = 2, n = 1-5$) in Figure 2 (b) could also, however, come from the ionization of the intermediates, such as ethane association products, shown in the hydrogenation reaction paths. Nonetheless, the
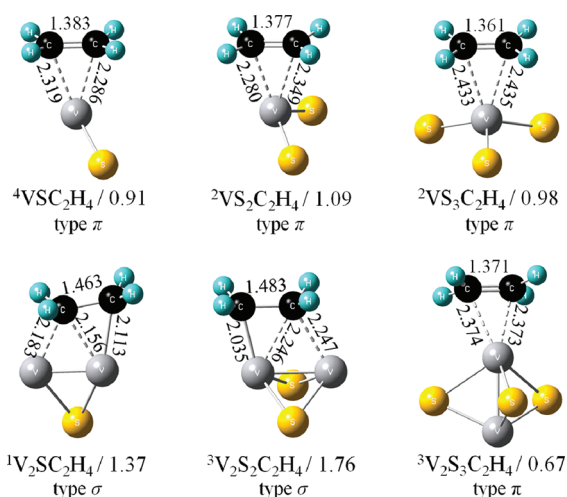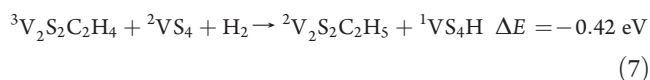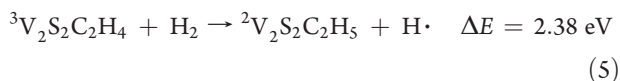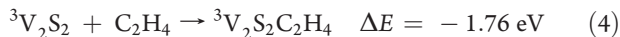
Figure 6. DFT optimized geometries of association products $^MV_{1,2}S_{1-3}C_2H_4$. Two types of geometry configurations (π and σ) are presented. For each cluster, only the lowest energy structure with spin multiplicity (M) is listed. The value in eV below the geometry is the zero-point vibrational energy corrected binding energies (the BSSE corrections are ignored as less than 10%). The C−C and V−C bond length values in Å are given.

Figure 7. Spin density profiles for $^MVS_{1-3}C_2H_4$ and $^MV_2S_2C_2H_4$ clusters. The superscript M indicates the spin multiplicity.

product $V_mS_nC_2H_6$ is the most stable one and will have the longest lifetime in the reaction. Products $V_mS_nC_2H_5$ and V_mS_nH are also observed (see Table 1) when V_mS_n clusters react with $C_2H_4 + H_2$ in the fast flow reactor (at ca. 300−400 K). The related possible reaction energies are calculated by DFT, such as

$$^3V_2S_2 + C_2H_4 \rightarrow {}^3V_2S_2C_2H_4 \quad \Delta E = -1.76 \text{ eV} \quad (4)$$

$$^3V_2S_2C_2H_4 + H_2 \rightarrow {}^2V_2S_2C_2H_5 + H\cdot \quad \Delta E = 2.38 \text{ eV} \quad (5)$$

$$^2VS_4 + H_2 \rightarrow {}^1VS_4H + H\cdot \quad \Delta E = 1.51 \text{ eV} \quad (6)$$

$$^3V_2S_2C_2H_4 + {}^2VS_4 + H_2 \rightarrow {}^2V_2S_2C_2H_5 + {}^1VS_4H \quad \Delta E = -0.42 \text{ eV} \quad (7)$$

$$2{}^2VS_4 + H_2 \rightarrow 2{}^1VS_4H \quad \Delta E = -1.29 \text{ eV} \quad (8)$$

Hydrogen radical generation is unfavorable for the reactions 5 and 6. Moreover, on the basis of our referenced studies of metal oxide clusters and their reactions with hydrocarbon compounds,[48−51] neutral V_mS_n and corresponding product ($V_mS_nH_2$ and $V_mS_nC_2H_6$) clusters should not fragment under 118 nm (10.5 eV) ionization. A single 10.5 eV photon is energetic enough to ionize these neutral clusters, and at about 0.5 μJ/pulse ($10^{11}-10^{12}$ photons/pulse at 118 nm), the probability that any cluster will absorb more than one photon is vanishingly small. Observation of series products $V_mS_nC_2H_5$ and V_mS_nH (see Figure 2b and Table 1) suggests that the reaction mechanism may involves multiple molecular collisions, such as given for reactions 7 and 8. These reactions are likely to occur in the reactor, because products $V_2S_2C_2H_5$ and VS_4H are both observed in Figure 2b. Multiple molecular collision reactions are also observed in our previous studies: for reactions of neutral iron oxide clusters with methanol,[49] products $(CH_2O)FeOH$ and FeOH
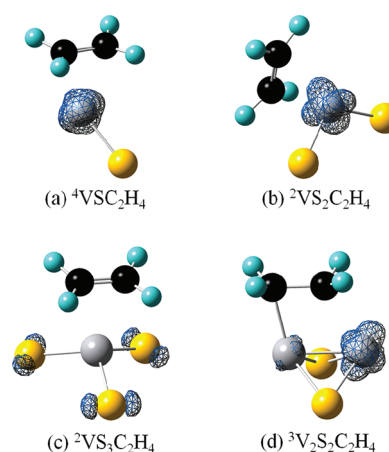
are both observed due to multiple molecule collision reactions (e.g., 2FeO + CH_3OH); and odd hydrogen atoms on the other cluster system, $M_mC_nH_x$ (M = Al, Be, Mg),[62,63] are also observed. Similarly, observation of other products $V_mS_nC_2H_5$ and V_mS_nH (Table 1) can also be understood in the same manner as above for $V_2S_2C_2H_5$ and VS_4H. Ethyl species are also observed as a stable intermediate in the study of ethylene hydrogenation on Pt surfaces during the hydrogenation process.[13]

As the calculation results for the reaction pathways of ethylene hydrogenation on VS_{1-3} and V_2S_2 clusters (shown in Figures 3−5) indicate, C_2H_4 is adsorbed on V atoms of these V_mS_n clusters in the first step of the reaction. The lowest energy structures of the association products $V_{1,2}S_{1-3}C_2H_4$ (shown in Figure 6) also indicate that the ethylene connects with $V_{1,2}S_{1-3}$ through V atoms. These results suggest that the V atoms of the catalytic V_mS_n clusters are the active sites for adsorption of ethylene. In the experimental results (Table 1), ethylene association products are observed on sulfur poor V_mS_n clusters, such as VS, VS_2, V_2S, V_2S_2, and so on, but are not observed on sulfur rich clusters, such as VS_4, VS_5, V_2S_6, and so on. Two possible explanations can rationalize these results. First, steric effects due to many S atoms bonding to V atoms in sulfur rich V_mS_n clusters can result in reduced binding of ethylene to V. In other words, the collision probability of ethylene with V atoms will decrease with the increase of the number of S atoms bonding to the V atoms, yielding C_2H_4 association products more difficult to form on the sulfur rich V_mS_n clusters. Second, the binding energy of ethylene with sulfur-rich clusters becomes small: for example, the calculated binding energy ($\sim$0.7 eV) of C_2H_4 with VS_4 is less than that with VS_{1-3} ($\sim$1.0 eV, Figure 6). According to the classical Rice-Ramsberger-Kassel-Markus (RRKM) theory, $k_{\text{dissociation}} = (1 - E_{\text{bind}}/E)^{s-1}$, in which $E_{\text{activation}}$ is replaced by E_{bind}, the binding energy of ($VS_nC_2H_4$), and s is the number of modes for the cluster, a lower binding energy implies a faster dissociation rate constant and thus a shorter lifetime for the metastable initial association intermediate ($VS_nC_2H_4^*$). The $VS_4C_2H_4^*$ would more easily fall apart ($VS_4 + C_2H_4$) if no further reactions and/or collisions could remove its excess energy. The above analysis suggests that the additional S atoms surrounding V atoms will reduce the availability and stability of the active V-ethylene intermediates.

After C_2H_4 molecules adsorb on catalytic V_mS_n clusters, the next step of the hydrogenation reaction is H_2 molecule attack on

10272

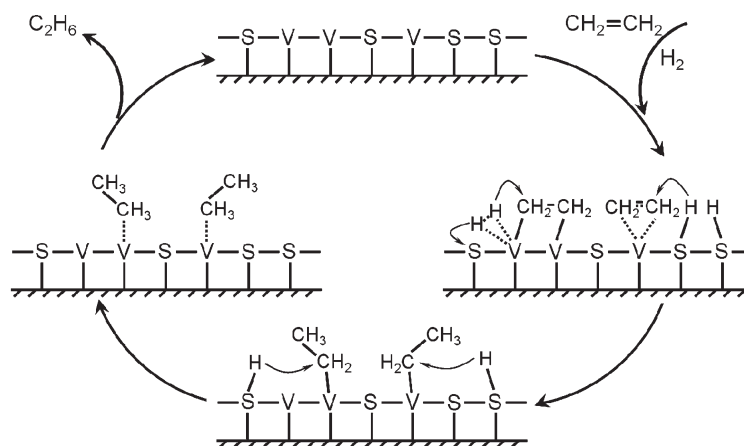dx.doi.org/10.1021/jp2056267 |*J. Phys. Chem. A* 2011, 115, 10266–10275

Figure 8. Proposed full catalytic cycle for the C_2H_4 hydrogenation reaction on a vanadium sulfide surface based on the calculations for the hydrogenation reaction of C_2H_4 on VS_{1-3} and V_2S_2 clusters.

the $V_mS_nC_2H_4$ cluster. Two different mechanisms for H_2 molecule dissociation on $V_mS_nC_2H_4$ can be found from the PESs calculation results (see Figures 3–5). From the spin density profiles for $VS_{1,2}C_2H_4$ and $V_2S_2C_2H_4$ in Figure 7, unpaired electrons are mostly localized on the V site, which is the most active site in the $VS_{1,2}C_2H_4$ and $V_2S_2C_2H_4$ clusters: the H_2 molecule can thus be adsorbed to these active V atoms of $VS_{1,2}C_2H_4$ and $V_2S_2C_2H_4$ clusters as given for reaction pathways presented in Figures 3 and 5. Then the H—H bond of the adsorbed H_2 ruptures: one of the H atom stays at the V atom site and forms a —VH group, and the other H atom transfers to an S atom and forms a —SH group. The reaction mechanism on the VS_3 cluster is different (Figure 4): the hydrogen molecule attaches to $VS_3C_2H_4$, and the H—H bond ruptures with a small barrier (~0.1 eV) to form two —SH groups on the S active sites directly. For the $VS_3C_2H_4$ cluster, the electrons are mostly localized on the S sites, as seen in the spin density profiles presented in Figure 7c. Although an approximate 0.1 eV barrier for breaking the H—H bond of H_2 directly on two adjacent sulfur atoms is present, this reaction is a reasonable one in the fast flow reactor based on thermodynamic considerations, taking into account DFT calculational uncertainties (about 0.2 eV); however, a higher barrier implies the reaction will be slower and thus the related product signal is weaker. From the experimental observations in Figure 2b, the intensity ratio of mass peak $VS_2C_2H_6$ to $VS_2C_2H_4$ is about 32%, whereas the ratio for $VS_3C_2H_6$ to $VS_3C_2H_4$ is only about 9%. The deduction from the calculation results is in good agreement with the experimental results.

In summary, our calculational and experimental results indicate that V atoms of catalytic V_mS_n clusters are the active sites for holding C_2H_4 molecules during the C_2H_4 hydrogenation reaction process; the H—H bond of H_2 molecule can either rupture after hydrogen absorption on active V sites or rupture directly on active S sites. The H_2 molecule is more easily dissociated on active V sites than on active S sites. The hydrogen atoms of either —VH and —SH groups can then transfer to ethylene to yield ethane in a stepwise process.

C. Understanding of the Condensed Phase Hydrogenation Reaction of Ethylene at a Molecular Level. A general hydrogenation mechanism by which ethylene is absorbed on a metal surface and hydrogenated by gas phase H_2 has been widely accepted for ethylene hydrogenation over metal surface.[27] The C_2H_4 hydrogenation mechanism on the vanadium sulfide surface,

however, has not been proposed previously. Studies for hydrogenation reactions of ethylene catalyzed by neutral vanadium sulfide clusters in the gas phase can aid in the understanding of the related condensed phase catalysis reaction at a molecular level. Catalytic clusters in gas phase can be seen as a good model system for the active moiety that exists on a catalyst surface. Thereby, a catalytic cycle for C_2H_4 hydrogenation on vanadium sulfide surfaces can be proposed, and is presented in Figure 8. This proposal is offered based on experimental and calculational results presented in Figures 2–5 and Table 1.

This suggested mechanism generally parallels that proposed by Horiuti and Polanyi for the reaction on a clean metal surface;[27] however, the cluster-based mechanism presents more important information about active sites on the catalytic surface. Compared to the mechanism proposed on the metal surface, this mechanism indicates that the C_2H_4 molecule adsorbs on the V site and reacts step by step with H atoms, which can be bound to either the V or the S site on the vanadium sulfide surface. The mechanism suggested from metal surface studies cannot supply the details of active sites on the catalytic surface.

We suggest that the V sites can be the active sites for neutral vanadium sulfide clusters to adsorb C_2H_4. The ethylene can either connect with one V site through its π orbital or form two σ bonds with two neighboring V sites (metal–metal bonding is also evident in condensed phase vanadium sulfides[64]). An H_2 molecule can either dissociate after attaching to an active V site or dissociate directly on active S sites. As discussed above, the dissociation of an H_2 molecule is also available through the multiple cluster molecule collision reactions. Because one catalytic cluster in the gas phase can represent an active moiety on the catalyst surface, the multiple cluster molecule collision reaction mechanism suggests that the rupture of the H—H bond of H_2 on two adjacent active moieties is a possible reaction process on catalytic surfaces: the H atoms, bonded to either a V or S site, can transfer stepwise to C_2H_4. Through an ethyl intermediate species, which bonds to an active V site, the ethane molecule can be formed and desorbed to the gas phase with the catalytic vanadium sulfide surface unchanged. The catalytic cycle (depicted in Figure 8) can give a more clear idea of vanadium sulfide catalyst surface behavior and, therefore, can help to understand the heterogeneous catalytic reaction mechanism on the condensed phase catalyst surface.

5. CONCLUSIONS

The hydrogenation reactions of C_2H_4 on neutral vanadium sulfide clusters are investigated by time-of-flight mass spectrometry employing 118 nm single photon ionization and DFT calculations. We find that the hydrogenation reactions of C_2H_4 are thermodynamically available on V_mS_n ($m = 1, n = 1-3; m = 2, n = 1-5$) clusters. The V atoms are the active sites for these V_mS_n clusters to attach a C_2H_4 molecule. Two types of association products for ethylene on active V sites of catalytic V_mS_n clusters are determined by DFT calculations. The C_2H_4 can connect with the active V atom through its π orbital or form a σ bond with active V atoms. Both π and σ associated ethylene can be hydrogenated with H_2 on catalytic V_mS_n clusters. PESs are calculated for hydrogenation reactions of C_2H_4 on the VS_{1-3}, V_2S_2 clusters. The H_2 molecule is predicted to be adsorbed on the V sites of $VS_{1,2}C_2H_4$ and $V_2S_2C_2H_4$ clusters and dissociate to form $-VH$ and $-SH$ groups. On the $VS_3C_2H_4$ cluster, the $H-H$ bond of the H_2 molecule ruptures directly on two adjacent S sites and forms $-SH$ groups. Theoretical calculations suggest that the reaction of the H_2 molecule on the $V_mS_nC_2H_4$ cluster is associated with electron density localized on different active sites. Sufficient electron spin density on V or S atoms is responsible for the adsorption or dissociation of H_2. The H atoms of $-VH$ and $-SH$ groups transfer to C_2H_4 step by step. The ethane molecule can be formed through an ethyl intermediate species which bonds to an active V site, and desorbs to the gas phase with the catalytic V_mS_n cluster unchanged. Additionally, all reactions are estimated as overall barrierless or with a small barrier (~0.1 eV), in thermodynamically favorable processes. A catalytic cycle for the hydrogenation reaction of C_2H_4 on a condensed phase vanadium sulfide catalyst surface is proposed based on the present gas phase cluster experimental and theoretical studies. The exposed V sites on a vanadium sulfide catalyst surface are suggested to be important for holding the C_2H_4 and H_2 molecules; S sites near an active V site are responsible for breaking the $H-H$ bond of the adsorbed H_2 molecule.

■ AUTHOR INFORMATION

Corresponding Author
*E-mail: erb@lamar.colostate.edu.

■ ACKNOWLEDGMENT

■ REFERENCES

(1) Stiefel, E. I., Matsumoto, K., Eds. *Transition Metal Sulfur Chemistry, Biological and Industrial Significance*; American Chemical Society: Washington, DC, 1997.

(2) Topøe, H., Clausen, B. S., Massoth, F. E., Eds. *Hydrotreating Catalysis: Science and Technology*; Springer Verlag: Berlin, 1996.

(3) Chianelli, R. R.; Daage, M.; Ledoux, M. J. *Adv. Catal.* **1994**, *40*, 177–232.

(4) Delmon, B. *Bull. Soc. Chim. Belg.* **1995**, *104*, 173–187.

(5) Ho, T. C. *Catal. Rev.—Sci. Eng.* **1988**, *30*, 117–160.

(6) Bond, G. C.; Wells, P. B. *Adv. Catal.* **1964**, *15*, 91–226.

(7) Cremer, P. S.; Somorjai, G. A. *J. Chem. Soc., Faraday Trans.* **1995**, *91*, 3671–3677.

(8) Mei, D. H.; Hansen, E. W.; Neurock, M. *J. Phys. Chem. B* **2003**, *107*, 798–810.

(9) Chen, Y.; Vlachos, D. G. *J. Phys. Chem. C* **2010**, *114*, 4973–4982.

(10) Moyes, R. B.; Walker, D. W.; Wells, P. B.; Whan, D. A.; Irvine, E. A. *Appl. Catal.* **1989**, *55*, L5.

(11) Adúriz, H. R.; Bodnariuk, P.; Dennehy, M.; Grgola, C. E. *Appl. Catal.* **1990**, *58*, 227–239.

(12) Stacchiola, D.; Burkholder, L.; Tysoe, W. T. *Surf. Sci.* **2002**, *511*, 215–228.

(13) Cremer, P. S.; Su, X.; Shen, R.; Somorjai, G. A. *J. Am. Chem. Soc.* **1996**, *118*, 2942–2949.

(14) Wang, L.; Tysoe, W. T. *J. Catal.* **1991**, *128*, 320–336.

(15) Tsung, C. K.; Kuhn, J. N.; Huang, W. Y.; Aliaga, C.; Hung, L. I.; Somorjai, G. A.; Yang, P. D. *J. Am. Chem. Soc.* **2009**, *131*, 5816–5822.

(16) Salciccioli, M.; Chen, Y.; Vlachos, D. G. *Ind. Eng. Chem. Res.* **2011**, *50*, 28–40.

(17) Stacchiola, D.; Burkholder, L.; Tysoe, W. T. *Surf. Sci.* **2002**, *511*, 215–228.

(18) Stacchiola, D.; Tysoe, W. T. *Surf. Sci.* **2002**, *513*, L431–L435.

(19) Stacchiola, D.; Tysoe, W. T. *Surf. Sci.* **2003**, *540*, L600–L604.

(20) Burkholder, L.; Stacchiola, D.; Tysoe, W. T. *Surf. Rev. Lett.* **2003**, *10*, 909–916.

(21) Zheng, T.; Stacchiola, D.; Poon, H. C.; Saldin, D. K.; Tysoe, W. T. *Surf. Sci.* **2004**, *564*, 71–78.

(22) Shaikhutdinov, Sh.; Heemeier, M.; Bäumer, M.; Lear, T.; Lennon, D.; Oldman, R. J.; Jackson, S. D.; Freund, H. J. *J. Catal.* **2001**, *200*, 330–339.

(23) Shaikhutdinov, Sh.; Frank, M.; Bäumer, M.; Jackson, S. D.; Oldman, R. J.; Hemminger, J. C.; Freund, H. J. *Catal. Lett.* **2002**, *80*, 115–122.

(24) Doyle, A. M.; Shaikhutdinov, S. K.; Jackson, S. D.; Freund, H. J. *Angew. Chem., Int. Ed.* **2003**, *42*, 5240–5243.

(25) Doyle, A. M.; Shaikhutdinov, S. K.; Freund, H. J. *J. Catal.* **2004**, *223*, 444–453.

(26) Dohnálek, Z.; Kim, J.; Kay, B. D. *J. Phys. Chem. C* **2008**, *112*, 15796–15801.

(27) Horiuti, J.; Polanyi, M. *Trans. Faraday Soc.* **1934**, *30*, 1164–1172.

(28) Stacchiola, D.; Azad, S.; Burkholder, L.; Tysoe, W. T. *J. Phys. Chem. B* **2001**, *105*, 11233–11239.

(29) Ogliaro, F.; Harris, N.; Cohen, S.; Filatov, M.; Visser, de, S. P.; Shaik, S. *J. Am. Chem. Soc.* **2000**, *122*, 8977–8989.

(30) Bohme, D. K.; Schwarz, H. *Angew. Chem., Int. Ed.* **2005**, *44*, 2336–2354.

(31) Zemski, K. A.; Justes, D. R.; Bell, R. C.; Castleman, A. W., Jr. *J. Phys. Chem. A* **2001**, *105*, 4410–4417.

(32) Schlangen, M.; Schroder, D.; Schwarz, H. *Angew. Chem., Int. Ed.* **2007**, *46*, 1641–1644.

(33) Bruin, B.; Budzelaar, P. H. M.; Wal, A. G. *Angew. Chem., Int. Ed.* **2004**, *43*, 4142–4157.

(34) Calatayud, M.; Mguig, B.; Miont, C. *Surf. Sci. Rep.* **2004**, *55*, 169–236.

(35) Asmis, K. R.; Brummer, M.; Kaposta, C.; Santambrogio, G.; von Helden, G.; Meijer, G.; Rademann, K.; Woste, L. *Phys. Chem. Chem. Phys.* **2002**, *4*, 1101–1104.

(36) Lacroix, M.; Boutarfa, N.; Guillard, C.; Vrinat, M.; Breysse, M. *J. Catal.* **1989**, *120*, 473–493.

(37) Guillard, C.; Lacroix, M.; Vrinat, M.; Breysse, M.; Mocaer, B.; Grimblot, J.; des Courieres, T.; Faure, D. *Catal. Today* **1990**, *7*, 587–600.

(38) Carlin, T. J.; Wise, M. B.; Freiser, B. S. *Inorg. Chem.* **1981**, *20*, 2743–2745.

(39) Dance, I.; Fisher, K.; Willett, G. *Angew. Chem., Int. Ed.* **1995**, *34*, 201–203.

(40) Dance, I. G.; Fisher, K. J.; Willett, G. D. *Inorg. Chem.* **1996**, *35*, 4177–4184.

(41) Kretzschmar, I.; Schroder, D.; Schwarz, H.; Rue, C.; Armentrout, P. B. *J. Phys. Chem. A* **1998**, *102*, 10060–10073.

(42) Kretzschmar, I.; Schroder, D.; Schwarz, H.; Armentrout, P. B. *Int. J. Mass. Spectrom.* **2003**, *228*, 439–456.

10274

dx.doi.org/10.1021/jp2056267 |*J. Phys. Chem. A* 2011, 115, 10266–10275

(43) Wang, W. J.; Liu, P.; Hu, D. B.; Gao, Z.; Kong, F. A.; Zhu, Q. H. *Chin. J. Chem. Phys.* **1997**, *10*, 110–116.

(44) Fisher, K.; Dance, I.; Willett, G.; Yi, M. N. *J. Chem. Soc., Dalton Trans.* **1996**, *5*, 709–718.

(45) Devore, T. C.; Franzen, H. F. *High Temp. Sci.* **1975**, *7*, 220–235.

(46) Ran, Q.; Tam, W. S.; Cheung, A. S. C.; Merer, A. J. *J. Mol. Spectrosc.* **2003**, *220*, 87–106.

(47) Liang, B. Y.; Andrews, L. *J. Phys. Chem. A* **2002**, *106*, 3738–3743.

(48) He, S. G.; Xie, Y.; Guo, Y. Q.; Bernstein, E. R. *J. Chem. Phys.* **2007**, *126*, 194315/1–194315/9.

(49) Xie, Y.; Dong, F.; Heinbuch, S.; Rocca, J. J.; Bernstein, E. R. *J. Chem. Phys.* **2009**, *130*, 114306/1–114306/11.

(50) Xue, W.; Wang, Z. C.; He, S. G.; Xie, Y.; Bernstein, E. R. *J. Am. Chem. Soc.* **2008**, *130*, 15879–15888.

(51) He, S. G.; Xie, Y.; Dong, F.; Heinbuch, S.; Jakubikova, E.; Rocca, J. J.; Bernstein, E. R. *J. Phys. Chem. A* **2008**, *112*, 11067–11077.

(52) Geusic, M. E.; Morse, M. D.; O'brien, S. C.; Smalley, R. E. *Rev. Sci. Instrum.* **1985**, *56*, 2123–2130.

(53) Becke, A. D. *Phys. Rev. A: At., Mol., Opt. Phys.* **1988**, *38*, 3098–3100.

(54) Perdew, J. P.; Wang, Y. *Phys. Rev. B: Condens. Matter* **1992**, *45*, 13244–13249.

(55) Frisch, M. J.; Trucks, G. W.; Schlegel, H. B.; Scuseria, G. E.; Robb, M. A.; Cheeseman, J. R.; Scalmani, G.; Barone, V.; Mennucci, B.; Petersson, G. A.; Nakatsuji, H.; Caricato, M.; Li, X.; Hratchian, H. P.; Izmaylov, A. F.; Bloino, J.; Zheng, G.; Sonnenberg, J. L.; Hada, M.; Ehara, M.; Toyota, K.; Fukuda, R.; Hasegawa, J.; Ishida, M.; Nakajima, T.; Honda, Y.; Kitao, O.; Nakai, H.; Vreven, T.; Montgomery, J. A.; Peralta, J. E., Jr.; Ogliaro, F.; Bearpark, M.; Heyd, J. J.; Brothers, E.; Kudin, K. N.; Staroverov, V. N.; Kobayashi, R.; Normand, J.; Raghavachari, K.; Rendell, A.; Burant, J. C.; Iyengar, S. S.; Tomasi, J.; Cossi, M.; Rega, N.; Millam, J. M.; Klene, M.; Knox, J. E.; Cross, J. B.; Bakken, V.; Adamo, C.; Jaramillo, J.; Gomperts, R.; Stratmann, R. E.; Yazyev, O.; Austin, A. J.; Cammi, R.; Pomelli, C.; Ochterski, J. W.; Martin, R. L.; Morokuma, K.; Zakrzewski, V. G.; Voth, G. A.; Salvador, P.; Dannenberg, J. J.; Dapprich, S.; Daniels, A. D.; Farkas, O.; Foresman, J. B.; Ortiz, J. V.; Cioslowski, J.; Fox, D. J. *Gaussian 09*, Revision A.02; Gaussian, Inc.: Wallingford, CT, 2009.

(56) Boys, F.; Benardi, F. *Mol. Phys.* **1970**, *19*, 553–566.

(57) Rappe, A. K.; Bernstein, E. R. *J. Phys. Chem. A* **2000**, *104*, 6117–6128.

(58) Cassuto, A.; Kiss, J.; White, J. *Surf. Sci.* **1991**, *255*, 289–294.

(59) Griffiths, K.; Lennard, W.; Mitchell, I.; Norton, P.; Pirug, G.; Bonzel, H. *Surf. Sci. Lett.* **1993**, *284*, L389–393.

(60) Cremer, P.; Stanners, C.; Niemantsverdriet, J.; Shen, Y.; Somorjai, G. *Surf. Sci.* **1995**, *328*, 111–118.

(61) Mohsin, S.; Trenary, M.; Robota, H. *J. Phys. Chem.* **1988**, *92*, 5229–5233.

(62) Dong, F.; Xie, Y.; Bernstein, E. R. *J. Chem. Phys.* **2011**, *135*, 054307/1−054307/6.

(63) Dong, F.; Heinbuch, S.; Xie, Y.; Rocca, J. J.; Bernstein, E. R. *Phys. Chem. Chem. Phys.* **2010**, *12*, 2569–2581.

(64) England, W. B.; Liu, S. H.; Myron, H. W. *J. Chem. Phys.* **1974**, *60*, 3760–3766.